Large Increase in Magnetoresistance and Cluster-Glass Behavior in Defect $Tl_{2-x}Mn_2O_{7-y}$ Pyrochlores

J. A. Alonso, M. J. Martínez-Lope, M. T. Casais, and J. L. Martínez*

Instituto de Ciencia de Materiales de Madrid (CSIC), Cantoblanco, E-28049 Madrid, Spain

M. T. Fernández-Díaz

Institut Laue-Langevin, BP 146X, F-38042 Grenoble Cedex 9, France

Received December 15, 1999. Revised Manuscript Received January 24, 2000

Moderate-pressure techniques ($P = 20$ kbar) have been used to prepare defect $Tl_{2-x}Mn_2O_{7-y}$ pyrochlore-like materials: Neutron powder diffraction (NPD) data show that a unique stoichiometry $Tl_{1.94}Mn_2O_{6.96}$ is stabilized under the present synthesis conditions. The defective character of these pyrochlores has a strong influence on the transport and magnetic properties. Both electrical resistance and magnetoresistance are enhanced with respect to reported data for stoichiometric $Tl_2Mn_2O_7$, as a consequence of the spin scattering introduced by Tl vacancies. The charge carriers are electrons, and the value obtained from the high-field Hall effect is 9.3×10^{-4} e^-/unit cell at 5 K. At the same time, a spin-glass behavior develops, subjacent to ferromagnetism, because of the weakening of the ferromagnetic (FM) interactions between near-neighbor Mn^{4+} cations. The observation by NPD of a distinct maximum at $Q \approx 0$ suggests the existence of FM clusters near room temperature (RT), vanishing below T_C to give a long-range-ordered ferromagnetic matrix.

I. Introduction

The discovery of magnetoresistance (MR) in manganese oxides[1−3] has aroused much interest, not only because of its technological implications but also because of the fascinating features and mechanism of the phenomenon in these materials. The prototypical colossal magnetoresistance (CMR) material is derived from the parent perovskite $LaMnO_3$, when holes are introduced, for instance, by Ca or Sr substitution for La, in $La_{1-x}A_xMnO_3$ (A = alkaliearth). CMR is observed in these manganites when they become ferromagnetic (FM) and transform from an insulating state to a metallic state near the Curie temperature (T_C). The overall features of MR in manganites can be understood on the basis of the double-exchange mechanism,[4] which accounts for both FM behavior and metallic conductivity below T_C. In addition, unusual magnetoelastic effects and charge ordering have focused attention on strong electron−phonon coupling. This coupling, which is a type of dynamic extended-system version of the Jahn−Teller effect, in conjunction with the double-exchange interaction, is also viewed as essential for a microscopic description of CMR in the manganite perovskites.[5,6] However, the observation of CMR in $Tl_2Mn_2O_7$,[7,8] with the pyrochlore structure, shows a different phenomenology: it has not been described a Mn^{3+}−Mn^{4+} mixed valence, which could account for Jahn−Teller-like distortions in the MnO_6 octahedra,[9,10] and there is no structural anomaly associated with the change in magnetotransport properties at 142 K, suggesting weak spin−lattice and charge−lattice correlations.[11] Instead of double exchange, a superexchange-type interaction between Mn^{4+} magnetic moments has been suggested to be responsible for the FM ordering of Mn spins,[11] whereas the metallic conductivity is thought to come from the overlap between Mn t_{2g}, O 2p, and Tl 6s block bands, resulting in a partial filling of the Tl 6s block bands.[12−14] This model for metallic conductivity of $Tl_2Mn_2O_7$ is coherent with the fact that $A_2Mn_2O_7$ pyrochlores are insulators when A = rare earth, Y, Sc, or In. All of these compounds show spontaneous magnetization at low temperatures, indicating FM transitions. Detailed ac and dc susceptibility as well as neutron diffraction studies do not provide any evidence for long-

(1) von Helmholt, R.; Wecker, J.; Holzapfel, B.; Schultz, L.; Samwer, K. *Phys. Rev. Lett.* **1993**, *71*, 2331.
(2) Jin, S.; O'Brian, H. M.; Tiefel, T. H.; McCormack, M.; Fastnacht, R. A.; Ramesh, R.; Chen, L. H. *Science* **1994**, *264*, 423.
(3) Ramirez, A. P. *J. Phys.: Condens. Matter* **1997**, *9*, 8171 and references therein.
(4) Zener, C. *Phys. Rev.* **1951**, *82*, 403. de Gennes, P.-G. *Phys. Rev.* **1960**, *118*, 141.
(5) Millis, A. J.; Shraiman, B. I.; Müeller, R. *Phys. Rev. Lett.* **1996**, *77*, 175.
(6) Roeder, H.; Hang, J.; Bishop, A. R. *Phys. Rev. Lett.* **1996**, *76*, 1356.
(7) Shimikawa, Y.; Kubo, Y.; Manako, T. *Nature* **1996**, *379*, 53.
(8) Subramanian, M. A.; Toby, B. H.; Ramirez, A. P.; Marshall, W. J.; Sleight, A. W.; Kwei, G. H. *Science* **1996**, *273*, 81.
(9) Rosenfeld, H. D.; Subramanian, M. A. *J. Solid State Chem.* **1996**, *125*, 278.
(10) Kwei, G. H.; Booth, C. H.; Bridges, F.; Subramanian, M. A. *Phys. Rev. B* **1997**, *55*, 688.
(11) Shimikawa, Y.; Kubo, Y.; Manako, T.; Sushko, Y. V.; Argyriou, D. N.; Jorgensen, J. D. *Phys. Rev. B* **1997**, *55*, 6399.
(12) Seo, D.-K.; Whangbo, M.-H.; Subramanian, M. A. *Solid State Commun.* **1997**, *101*, 417.
(13) Singh, D. J. *Phys. Rev. B* **1997**, *55*, 313.
(14) Ventura, C. I.; Alascio, B. *Phys. Rev. B* **1997**, *56*, 14533.
(15) Subramanian, M. A.; Greedan, J. E.; Raju, N. P.; Ramirez, A. P.; Sleight, A. W. *J. Phys. IV France* **1997**, *7*, 625.

10.1021/cm9911924 CCC: $19.00
Published on Web 03/24/2000

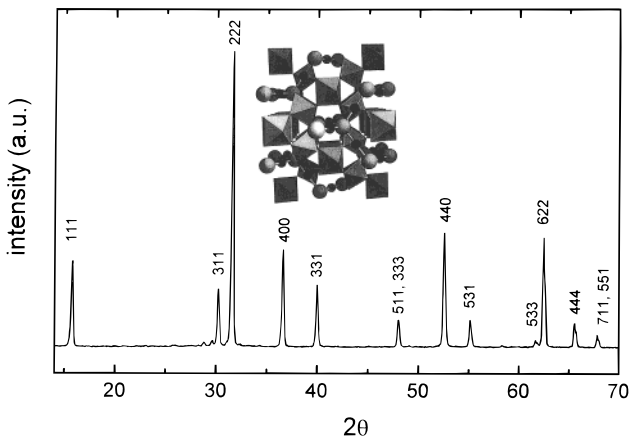

Figure 1. XRD pattern for $Tl_{1.94}Mn_2O_{6.96}$, indexed in a cubic unit cell with $a = 9.8909(1)$ Å. In the inset, a view of the pyrochlore structure, showing the vertex-sharing network of MnO_6 octahedra and the independent Tl−O′ sublattice (dark (Tl) and light (O′) spheres).

range ordering in $A_2Mn_2O_7$ phases where A is a rare earth, Y, Sc, or In but suggest a reentrant spin-glass-like behavior.[15] However, neutron powder diffraction (NPD) investigations substantiate the long-range magnetic ordering for $Tl_2Mn_2O_7$.[11,16]

The pyrochlore structure, of general stoichiometry $A_2B_2O_6O'$, can be described as two interpenetrating networks.[17] The smaller B cations are octahedrally coordinated to O-type oxygens, with the BO_6 octahedra sharing corners to give a B_2O_6 sublattice, which can be considered as the backbone of the structure (see inset of Figure 1). The cagelike holes of this network contain a second sublattice A_2O', not essential for the stability of the structure: both A and O′ atoms may be partially or totally absent, as happens in certain families of defect pyrochlores AB_2O_6.[17] As in most pyrochlores, $Tl_2Mn_2O_7$ oxide crystallizes in the cubic space group $Fd\bar{3}m$ (No. 227). When the origin is set at $\bar{3}m$, the structure can be described with Tl cations distributed at random at 16c (0, 0, 0) positions, Mn cations at 16d ($^1/_2$, $^1/_2$, $^1/_2$), O at 48f (u, $^1/_8$, $^1/_8$), and O′ at 8a ($^1/_8$, $^1/_8$, $^1/_8$) positions.

Here we study the effect of introducing Tl and O′ vacancies in $Tl_{2-x}Mn_2O_{7-y}$ with the pyrochlore structure. We have been able to prepare single-phased pyrochlores with significant Tl deficiency, observing that Tl vacancies are accompanied by O′ vacancies. We found that the creation of Tl (and O′) vacancies has a dramatic effect on both electronic transport and magnetotransport: the magnetoresistance MR(H), defined as $100[R(0) - R(H)]/R(H)$, increases by a factor of 5 at 150 K and is substantially higher at room temperature (RT), with respect to stoichiometric $Tl_2Mn_2O_7$. At the same time, ac susceptibility data show features characteristic of spin-glass systems. Finally, NPD data suggest the existence of magnetic clusters of spin-polaronic nature between RT and T_C, which support previous ideas pointing to the existence of a component of phonon-assisted conductivity in Tl pyrochlores.

II. Experimental Section

Samples of nominal stoichiometry $Tl_2Mn_2O_7$ were prepared under high-pressure conditions. About 1.5 g of a stoichiometric mixture of Tl_2O_3 and MnO_2, oxides were thoroughly ground and put into a gold capsule (8 mm diameter), sealed, and placed in a cylindrical graphite heater. The reaction was carried out in a piston−cylinder press (Rockland Research Co.), at a pressure of 20 kbar at 1000 ° C for 1 h. Then the material was quenched to RT, and the pressure was subsequently released. The raw products, obtained as dense, homogeneous pellets, were partially ground to perform the structural and magnetic characterization; some as-grown pellets were kept for the magnetotransport measurements.

The products were initially characterized by X-ray diffraction (XRD) for phase identification and for assessment of phase purity. For the structural refinements, NPD patterns for three samples, prepared in three independent runs, were collected at RT in a D2B high-resolution neutron diffractometer of ILL, Grenoble (France). The high-flux mode was selected, given the relatively small amount of sample available (about 800 mg for each sample). A wavelength of 1.594 Å was employed. The thermal evolution of NPD patterns was studied in a D1B diffractometer, with $\lambda = 2.52$ Å, between 1.5 and 300 K. NPD data were refined by the Rietveld[18] method, using the FULLPROF refinement program.[19] A pseudo-Voigt function was chosen to generate the line shape of the diffraction peaks. No regions were excluded in the refinement. In the final run the following parameters were refined: scale factor, background coefficients, zero-point error, unit-cell parameter, pseudo-Voigt corrected for asymmetry parameters, positional coordinates (u for O oxygen), isotropic thermal factors, and occupancy factors for Tl and O′ oxygen.

The dc and ac magnetizations were measured with a commercial SQUID magnetometer on powdered samples; transport and magnetotransport measurements were performed by the conventional four-probe technique on as-grown sintered pellets, under magnetic fields up to 9 T. Specific heat measurements have been carried out in the temperature range 2−300 K by the heat pulse relaxation method, under applied external magnetic fields up to 9 T, in a Physical Properties Measurement System (PPMS, from Quantum Design, San Diego, CA).

III. Results and Discussion

The materials were characterized by XRD as a single-phased pyrochlore, as illustrated in Figure 1. All of the reflections could be indexed in a cubic unit cell, with a lattice parameter $a = 9.8909(1)$ Å. Because the XRD scattering factors of Tl and Mn are considerably higher than that of oxygen, neutron diffraction techniques were necessary to complement the XRD data in order to extract accurate structural information concerning metal-to-oxygen distances, Mn−O−Mn, angles and other structural features. The results of refinement of the NPD data of three independently prepared samples

(16) Shimakawa, Y.; Kubo, Y.; Hamda, N.; Jorgensen, J. D.; Zu, Z.; Short, S.; Nohara, N.; Takagi, H. *Phys. Rev. B* **1999**, *59*, 1249.
(17) Subramanian, M. A.; Aravamudan, G.; Subba Rao, G. V. *Prog. Solid State Chem.* **1983**, *15*, 55.
(18) Rietveld, H. M. *J. Appl. Crystallogr.* **1969**, *2*, 65.
(19) FULLPROF: Rodríguez-Carvajal, J. *Physica B* **1993**, *192*, 55.

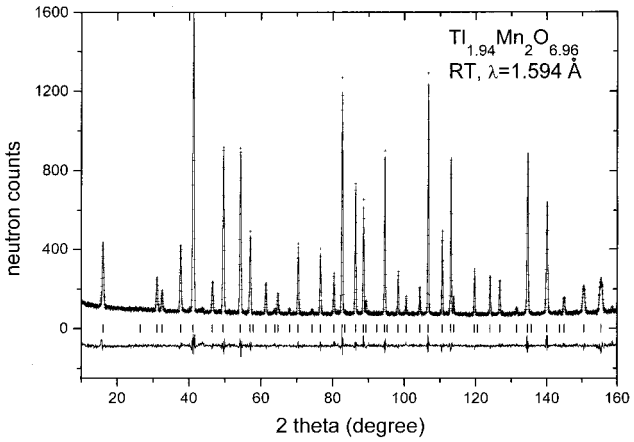

Figure 2. Observed (crosses), calculated (solid line), and difference (below) NPD profiles after the Rietveld refinement of $Tl_{1.94}Mn_2O_{6.96}$ structure at RT.

Table 1. Structural Parameters for $Tl_{1.94}Mn_2O_{6.96}$ after the Rietveld Refinement of NPD Data at RT (Space group $Fd\bar{3}m$, $Z = 8$, $a = 9.89094(6)$ (Å). Reliability Factors $\chi^2 = 1.74$, $R_p = 3.97$, $R_{wp} = 5.14$, $R_{exp} = 3.90$, $R_I = 1.79$)

atom	site	*x*	*y*	*z*	f_{occ}	B_{eq} (Å^2)
Tl	16c	0	0	0	0.972(3)	0.65(2)
Mn	16d	0.5	0.5	0.5	1.0	0.40(3)
O1	48f	0.4245(8)	0.125	0.125	1.0	0.63(2)
O2	8a	0.125	0.125	0.125	0.964(6)	0.44(4)

crystallographic formula	$Tl_{1.944(6)}Mn_2O_{6.96(1)}$
anisotropic thermal factors ($\times 10^4$)	
Tl	$\beta_{11} = \beta_{22} = \beta_{33} = 16.7(5)$
	$\beta_{12} = \beta_{13} = \beta_{23} = -3.1(6)$
Mn	$\beta_{11} = \beta_{22} = \beta_{33} = 10.1(8)$
	$\beta_{12} = \beta_{13} = \beta_{23} = -1.1(13)$
O1	$\beta_{11} = \beta_{22} = 18(1)$, $\beta_{33} = 12(1)$
	$\beta_{12} = 5(2)$, $\beta_{13} = \beta_{23} = -5(1)$
O2	$\beta_{11} = \beta_{22} = \beta_{33} = 11(1)$
	$\beta_{12} = \beta_{13} = \beta_{23} = 0$

were in complete agreement. The final atomic coordinates, unit-cell parameters, and discrepancy factors are given in Table 1. Figure 2 illustrates the goodness of fit.

The refinement of the occupancy factors for Tl and O′ led to a stoichiometry significantly deficient in both atomic positions: $Tl_{1.944(6)}Mn_2O_6O'_{0.96(1)}$. The nominal valence for Mn is +4.04(3) (assuming a trivalent state for Tl cations and a divalent state for oxygen anions), close to the expected value of +4, because Tl deficiency is coupled with O′ deficiency. Our results suggest the absence of a nominal mixed valence on the Mn sublattice, as previously reported.[8−10] However, at variance with previous reports,[8,11] we describe some significant deficiency at both Tl and O′ positions. This result can have strong implications concerning the mechanism for electronic conduction in this pyrochlore, as discussed later.

In the final refinement, we considered full anisotropic thermal parameters for all of the atoms in the unit cell. Other previous refinements considering isotropic thermal motion or stoichiometric occupancy for Tl and O2 positions always led to significantly worse discrepancy *R* factors, as shown in Table 2. To be noted is the good agreement obtained for Tl and O2 occupancy factors in both isotropic and anisotropic refinements.

Table 3 lists the main interatomic bond lengths and angles. The Mn−O distance observed for $Tl_{1.944(6)}Mn_2O_6O'_{0.96(1)}$, of 1.9013(4) Å, is also in agreement with previously reported values, of 1.9034(6) Å in ref 11, also refined from NPD data. Mn−O−Mn angles, of 133.74(1)°, are also comparable with those reported for stoichiometric $Tl_2Mn_2O_7$, of 133.44(8)°.

Table 2. Comparison between Final Discrepancy Factors for Various Refinement Models[a]

model[a]	R_p	R_{wp}	χ^2	R_I	f_{occ}(Tl)	f_{occ}(O2)
a	4.13	5.31	1.85	2.69	1.0	1.0
b	4.05	5.25	1.81	2.15	0.972(3)	0.960(6)
c	4.03	5.22	1.79	2.21	1.0	1.0
d	3.97	5.14	1.74	1.79	0.972(3)	0.964(6)

[a] Models: (a) isotropic; occupancy factors fixed to unit; (b) isotropic; occupancy factors refined; (c) anisotropic; occupancy factors fixed to unity; (d) anisotropic; occupancy factors refined.

Table 3. Main Interatomic Bond Distances (Å) and Angles (deg) for $Tl_{1.94}Mn_2O_{6.96}$ at RT

Mn−O1 (×6)	1.9013(4)	Tl−O (×6)	2.4568(4)
Mn−O1−Mn	133.74(1)	Tl−O′ (×2)	2.14146(1)

The magnetization vs temperature data (Figure 3) show a low-temperature saturation for $Tl_{1.94}Mn_2O_{6.96}$ characteristic of the spontaneous FM ordering described earlier.[7,8] The magnetization vs magnetic field data at 5 K shown in the inset of Figure 3 are characteristic of a ferromagnet with a saturation magnetic moment of 2.65 μ_B per Mn ion (close to that expected for Mn^{4+} of 3.0 μ_B). However, the presence of irreversibilities (differences between field-cooled (FC) and zero-field-cooled (ZFC) curves) already suggests that the magnetic properties of $Tl_{1.94}Mn_2O_{6.96}$ are more complex than those of a simple ferromagnet and display the existence of antiferromagnetic (AFM) interactions competing with the net ferromagnetism, as already proposed in this family of compounds.[20−22] The ac magnetic measurements give evidence for a cluster-glass-like behavior subjacent to ferromagnetism. Figure 4 shows the variation of real and imaginary parts of the susceptibility with temperature. The existence of a plateau in χ' at relatively high temperatures (115−130 K), strongly frequency dependent, suggests the presence of antagonistic interactions before the establishment of a net FM ordering below 115 K; in the same temperature range the maximum in χ'' corresponding to the FM ordering is surprisingly broad, and the presence of a second weak maximum at 40 K seems to correspond to the crystallization of a cluster-glass state, which should be better named as a *reentrant* cluster-glass system.[23] As is characteristic for spinglasses, the cusp temperature has been found to depend on the ac frequency. A cluster-glass behavior has been recently described for the $Tl_{2-x}Bi_xMn_2O_7$ pyrochlore series.[24]

In our defective samples, the cluster-glass effect can be associated with the presence of vacancies in both Tl

(20) Sushko, Y. V.; et al. *Rev. High Pressure Sci. Technol.* **1998**, *7*, 505. See also: Sushko, Y. V.; et al. *Physica B* **1999**, *259−261*, 831.
(21) Martínez, B.; Senis, R.; Fontcuberta, J.; Obradors, X.; Cheik-Rouhou, W.; Strobel, P.; Bougerol-Chaillot, C.; Pernet, M. *Phys. Rev. Lett.* **1999**, *83*, 2022.
(22) Alonso, J. A.; Martínez-Lope, M. J.; Casais, M. T.; Velasco, P.; Martínez, J. L.; Fernández-Díaz, M. T.; de Paoli, J. M. *Phys. Rev. B* **1999**, *60*, 15024.
(23) Gingras, M. J. P. In *Magnetic Systems with Competing Interaction*; Diep, H. T., Ed.; World Scientific Publishing Co.: Singapore, 1994; p 238.
(24) Alonso, J. A.; Martínez, J. L.; Martínez-Lope, M. J.; Casais, M. T.; Fernández-Díaz, M. T. *Phys. Rev. Lett.* **1999**, *82*, 189.

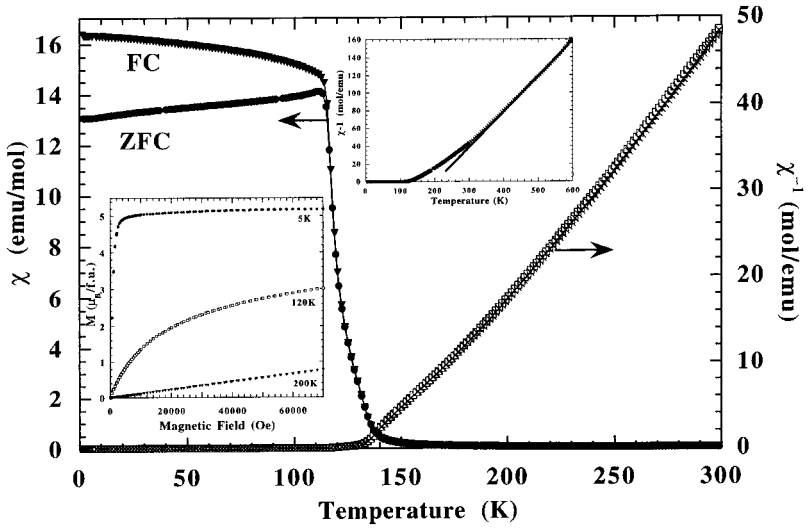

Figure 3. dc susceptiblity as a function of temperature showing zero-field-cooled (ZFC) and field-cooled (FC) curves for $Tl_{1.94}Mn_2O_{6.96}$. The upper inset shows the reciprocal susceptibility vs T (up to 600 K). The lower inset shows magnetization vs magnetic field at different temperatures.

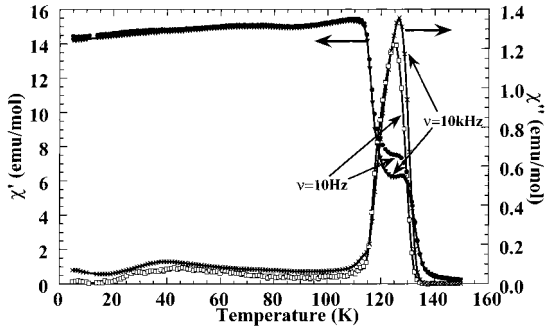

Figure 4. Real and imaginary part of the ac susceptibility as a function of temperature for $Tl_{1.94}Mn_2O_{6.96}$, at $\nu = 0.01$ and 10 kHz.

and O′ sublattices. It should be recalled that $A_2Mn_2O_7$ pyrochlores (A = Sc, Y, Ho, Yb, and Lu) exhibit[15] clear FC-ZFC irreversibilities, and ac susceptibility results indicate the presence of both near-neighbor AFM and FM (second- and third-neighbor) short-range correlations, in common with spin glasses. In $A_2Mn_2O_7$ pyrochlores the Mn atoms occupy the corners of a tetrahedra: spins at two points of the tetrahedron may couple in an antiparallel fashion, but it is impossible for the remaining two atoms to align their spins antiparallel to the first two. This high degree of geometrical frustration seems to be responsible for the complex magnetic behavior of these systems, in which ferromagnetism may dominate the magnetic interactions (as happens in stoichiometric $Tl_2Mn_2O_7$) or, through subtle structural changes, frustrated antiferromagnetism can progressively become apparent. On the other hand, Sushko et al.[20] have recently shown that the application of an external pressure suppresses ferromagnetism in $Tl_2Mn_2O_7$, which gives evidence against a simple FM superexchange picture, implying, instead, a more exotic scenario where the nearest-neighbor superexchange coupling is AFM, while ferromagnetism originates from the longer range interactions, which are generally weaker but could be dominant in pyrochlores because of geometrical frustration of AFM interactions. From the observation that $Tl_2Mn_2O_7$ and $In_2Mn_2O_7$ show significantly higher Curie temperatures than the remaining $A_2Mn_2O_7$ (A = rare earths and Sc) pyrochlores, these authors[20] suggest that the strong covalent bonding of Mn−O−Tl(In)−O−Mn may enhance the FM coupling, because both Tl and In have active 6s or 5s orbitals able to hybridize with O 2p orbitals. According to this picture, the partial absence of some Tl atoms from the structure, as observed in defect $Tl_{1.94}Mn_2O_{6.96}$, would result in a weakening of the FM interactions (mediated through Tl orbitals), thus enhancing the competition of AFM interactions finally leading to the observed cluster-glass behavior.

The inverse susceptibility $1/\chi$ follows a Curie−Weiss behavior only for temperatures well above T_C. Susceptibility data taken above RT (inset of Figure 3) are indicative of the existence of magnetic interactions below 350 K; the intermediate regime $T_C \leq T \leq 350$ K could be described as a spin−polaron state, in the framework of a recent model for a low-density electron gas coupled to FM spin fluctuations.[25] A paramagnetic moment (p) of 3.77 μ_B per manganese cation (expected for Mn^{4+}, 3.80 μ_B) is observed from the Curie−Weiss fit.

The transport and magnetotransport properties of $Tl_{1.94}Mn_2O_{6.96}$ are shown in Figure 5. To be noted is that a semiconducting behavior is observed above 200 K, instead of the metallic behavior described in this temperature regime for stoichiometric $Tl_2Mn_2O_7$. The resistivity ρ (300 K, $H = 0$) is also higher than that reported earlier[8] of about 10^{-1} Ω cm. This may be related to the presence of a significant number of Tl vacancies (0.06(1) atoms per formula unit), as discussed before. It should be recalled that the large electronic conductivity of $Tl_2Mn_2O_7$ is thought to be achieved through the mixing of the voluminous Tl 6s orbitals with O 2p and Mn 3d orbitals, in contrast with other insulating $A_2Mn_2O_7$ pyrochlores. The reduction in the concentration of Tl atoms introduces a strong-scattering 6s vacancy into the Tl−O network. Measurements of the high-field (H > 3T) Hall effect in these samples give a charge carrier density of 0.000 927 e^-/unit cell at 5 K,

(25) Majumdar, P.; Litlewood, P. *Phys. Rev. Lett.* **1998**, *81*, 1314. See also: Majumdar, P.; Litlewood, P. *Nature* **1998**, *395*, 479.

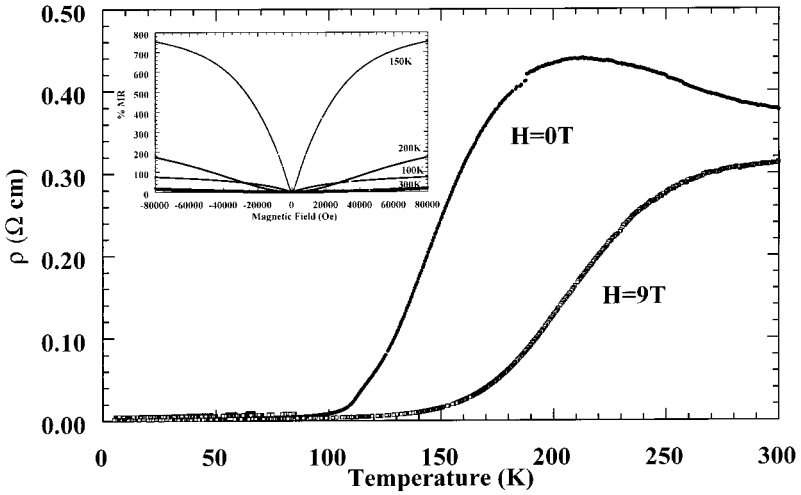

Figure 5. Resistivity vs temperature plots at $H = 0$ and 9 T, for $Tl_{1.94}Mn_2O_{6.96}$. The inset shows the field variation of MR at different temperatures for $Tl_{1.94}Mn_2O_{6.96}$. $MR(H) = 100[R(0) - R(H))/R(H)]$.

with some temperature dependence around T_C. This value should be compared with the data for the stoichiometric compound of 0.001−0.005 e^-/unit cell,[7] which indicate a clear decrease in the charge carrier in the defective samples.

However, the defective character of our $Tl_{1.94}Mn_2O_{6.96}$ sample is advantageous concerning the MR properties: as shown in the inset of Figure 5 a maximum MR(9 T) [defined as $MR(9\ T) = 100[R(0) - R(9\ T))/R(9\ T)]$ of 7.6 $\times 10^2$% is observed at 150 K, whereas the reported value for the stoichiometric pyrochlore (for 6 T) is at least 5 times lower.[7,8,26] With respect to this, the still more remarkable increase in MR observed by partial replacement of Tl by Sc[27] or Bi,[24] by a factor of 10^3, should be mentioned. A remarkable feature of defect $Tl_{1.94}Mn_2O_{6.96}$ lies in the RT behavior. As shown in the inset of Figure 5, the MR(9 T) value at 300 K is about 20%. This is comparable to the best results obtained for perovskite manganites, with large cations at the A positions, showing MR in the 10^2% range.[28] MR in pyrochlores was only described to occur below 200 K: the possibility of achievement of large MR at RT was only recently demonstrated in the $Tl_{1-x}Bi_xMn_2O_7$ series;[24] the present results show that defect compositions such as that found for $Tl_{1.94}Mn_2O_{6.96}$ may also enhance RT MR up to levels which make it possible to propose these materials as candidates for technical applications. After the Majumdar and Litlewood (ML) model,[25] the MR in the Tl family of compounds is related to the spin fluctuations and the low-density carrier in the system. From the ML model there is a direct relation between the magnetic fluctuations above T_C and the MR, $(\Delta\rho/\rho) = C(M/M_s)^2$, with the slope being $C = n^{-2/3}$. From the present data the calculated charge carrier value inside the ML model is $n = 0.0018$ e^-/unit cell, in fair agreement with the experimental value (1×10^{-3} e^-/unit cell). From the present data we can conclude that the qualitaive conclusions of the ML model are fulfilled in our case; the lower charge carrier density is related to the higher MR factors.

Figure 6 shows the thermal evolution of specific heat collected at different external fields, $H = 0$, 1, 3, and 9 T. A broad maximum centered at 112 K corresponds to the establishment of the long-range FM ordering, as is also observed by NPD. This peak shifts and spreads out under a magnetic field because of the reduction of entropy associated with the strong magnetization imposed by the external field. The inset shows the excess specific heat associated with the long-range FM ordering. These data were obtained after the subtraction of a phononic contribution, calculated by means of three Einstein oscillators at 120, 350, and 850 K. The entropy associated with this magnetic transition could be obtained as $\int(C/T)\,dT$ and gives 2.23 J mol^{-1} K^{-1} for $H = 0$.

Finally, we present data on the low-temperature evolution of the NPD patterns of $Tl_{1.94}Mn_2O_{6.96}$ is shown in Figure 7. A magnetic contribution on the low-angle reflections is observed below $T_C \leq 115$ K, corresponding to the establishment of long-range FM ordering, as expected and described earlier.[11] However, the most striking feature of the patterns is the presence of a broad maximum at $Q \approx 0$. This maximum is already present at RT and strongly decreases in intensity below T_C; therefore, we think it is associated with the existence of FM clusters which collapse at T_C to give a long-range-ordered FM matrix. This is true small-angle scattering, not the expected paramagnetic scattering that should be extended to higher angles, following the Mn^{4+} magnetic form factor. The half-width of this scattering extended only to low scattering angles is related to the size of the ferromagnetic clusters. The presence of magnetic interactions above T_C was already shown from susceptibility measurements (Figure 3). Given the AFM character proposed for the near-neighbor Mn−O−Mn interactions,[20] the geometrical frustration inherent to the Mn arrangement in the pyrochlore structure hinders the establishment of a long-range FM ordering at high temperatures, leading to the formation of FM clusters. These clusters are not able to collapse and condense in a FM matrix but at temperatures below T_C, at which the longer range FM interactions become dominant. Note that, nevertheless, the preponderance of FM interactions is not complete even at temperatures well

(26) Hwang, H. Y.; Cheong, S.-W. *Nature* **1997**, *289*, 942.
(27) Ramirez, A. P.; Subramanian, M. A. *Science* **1997**, *277*, 546.
(28) Khazeni, K.; Jia, Y. X.; Lu, L.; Crespi, V. H.; Cohen, M. L.; Zettl, A. *Phys. Rev. Lett.* **1996**, *76*, 295.

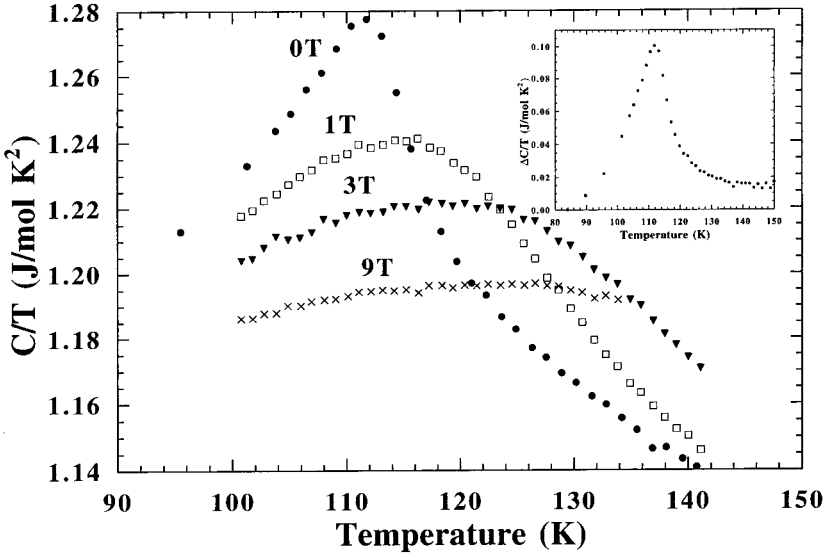

Figure 6. Specific heat data at different magnetic fields (H = 0, 1, 3, and 9 T) in a temperature range around T_C for $Tl_{1.94}Mn_2O_{6.96}$. The inset shows the magnetic specific heat ($\Delta C/T$) associated with the FM ordering.

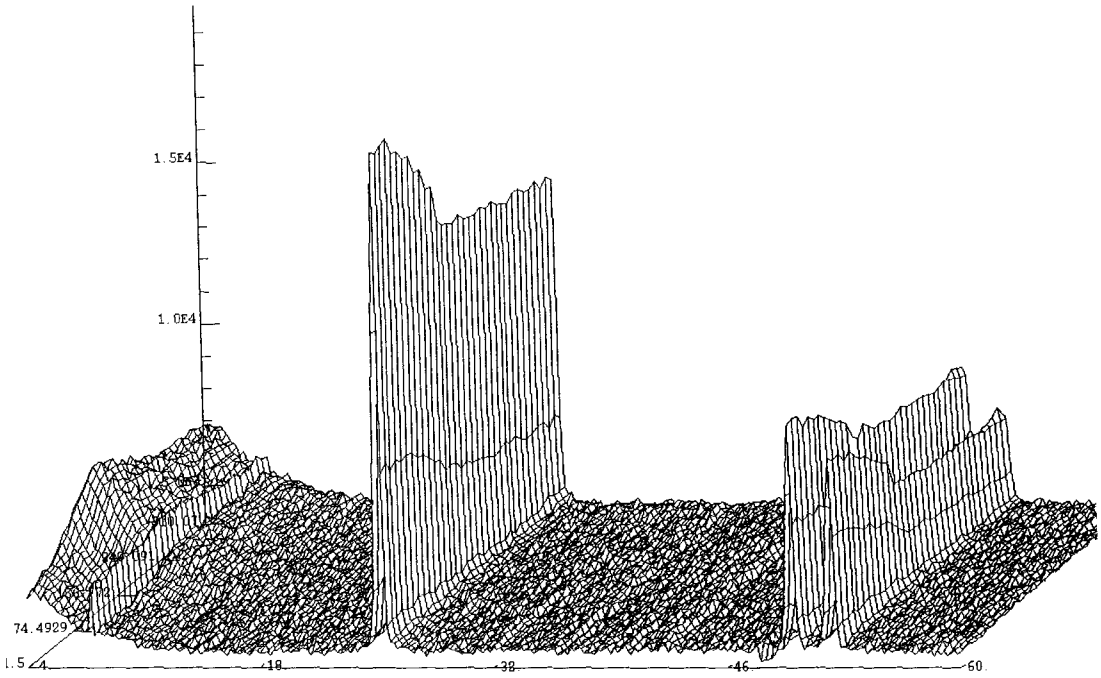

Figure 7. Temperature evolution of NPD patterns of $Tl_{1.94}Mn_2O_{6.96}$, with λ = 2.52 Å. The magnetic correlations are observed centered at $Q \approx 0$ in the low-angle region in a temperature region from 1.5 to 300 K.

below T_C, because a cluster-glass behavior is underlying ferromagnetism. This scenario is significantly different from that proposed for CMR perovskites, in which the presence of FM clusters associated with charge carriers and involving a deformation of the lattice (known as *magnetic polarons*) has been observed[29] in the paramagnetic region. In contrast, the existence of *magnetic polarons* seems not to be possible in the current scenario for $Tl_2Mn_2O_7$ pyrochlore, which considers a total absence of mixed valence for Mn cations and the undistorted character of MnO_6 octahedra. At present, we do not have any evidence for the coupling of the observed clusters with the charge carriers and/or any associated distortions of the crystal lattice in regions close to the clusters. We think that the existence of FM clusters (*spin polarons*), which had not been described before for the stoichiometric $Tl_2Mn_2O_7$ pyrochlore, is closely related to the defective character of $Tl_{1.94}Mn_2O_{6.96}$ oxide, in which the defective character of the Tl sublattice accounts for the weakening of the FM interactions and, thus, favors the competitive AFM interactions between Mn^{4+} moments.

IV. Conclusions

We have shown that moderate pressure synthesis techniques can be used to prepare $Tl_2Mn_2O_7$ materials with vacancies in both Tl and O′ sublattices. The crystallographic stoichiometry obtained from NPD data, $Tl_{1.94}Mn_2O_{6.96}$, suggests that Tl and O′ vacancies are coupled in such a way that the formal valence of Mn

(29) de Teresa, J. M.; et al. *Nature* **1997**, *386*, 256 and references therein.

remains close to +4. The defective character of these pyrochlores accounts for the observed increase in resistance, because the reduction in the concentration of Tl atoms introduces a strong-scattering 6s vacancy into the Tl−O network, and magnetoresistance enhanced up to 7.6×10^2% at 150 K and 20% at RT. Moreover, the partial absence of some Tl atoms from the structure results in a weakening of the FM interactions (mediated through Tl orbitals), thus enhancing the competition of AFM interactions and finally leading to the observation of a cluster-glass behavior. Low-temperature neutron diffraction shows evidence for the presence of FM clusters (*spin polarons*) even at temperatures close to RT, which vanish by cooling below T_C to give rise to a long-range ferromagnetically ordered matrix. The present results complement the current ideas on the exclusive role played by tallium atoms in the mechanism of metallic conductivity, highlighting the important role of subtle structural modifications, through the incorporation of moderate amounts of O′ and Tl vacancies, in the transport and magnetic properties of these defect pyrochlores.

Acknowledgment. We are thankful for the financial support of CICyT via Projects PB97-1181 and MAT99-1045, and we are grateful to ILL for making all facilities available. We also thank P. Velasco for help in the Hall effect measurements.

CM9911924